

# CEPC Draft

---

**Paper title**

**Version:** x.y

**To be submitted to:** Journal name

**Corresponding editor(s)**

---

**Comments are due by:** Comments deadline

---





## 1 Introduction

The discovery of Higgs boson by CMS and ATLAS experiments installed in LHC was one of the most important achievements in particle physics in recent years, finding the last missing piece of the standard model. It prompted physicists to study its various properties and their implications. However, as a hadron collider, the LHC's interaction area is highly messed up. Making it extremely difficult to probe the rare Higgs related events in detail. The CEPC on the other hand, is a  $e^+e^-$  collider, and thus provides a much cleaner environment. Enabling a resolution up to a hundred times more powerful than LHC and unambiguously determine Higgs self interaction and other behaviors, despite having smaller Higgs production rate.

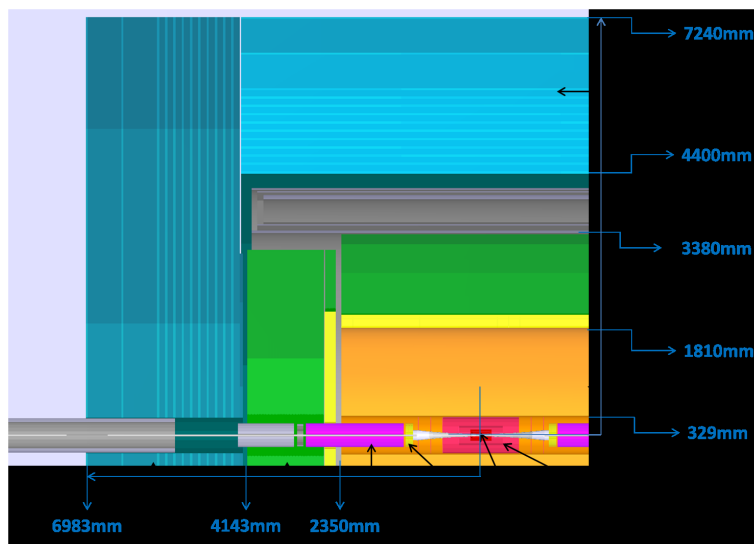


Figure 1: CEPC detector layout

The CEPC detector is based on ILC(International Linear Collider) detector, as shown in Figure 1. The SET subdetector is a thin layer of silicon detector situated in between the barrel area of TPC and Ecal(Electromagnetic Calorimeter). TPC is a gaseous tracker that's been widely used in high energy particle detectors because of its excellent tracking performance, simplicity, low cost, low material budget, pile up resistance and etc. The planned TPC resolution for CEPC is around  $100\mu\text{m}$ . The silicon detector on the other hand, is quite the opposite, except providing a resolution of a few micrometers. Thus the main purpose of SET is two fold, one is to provide precise entry point to the calorimeter, the other one is to improve overall tracking performance in the central region. In addition, it can be used to monitor any anomaly might happen in TPC. But the big area it needs to cover makes it very expensive and the position also poses tricky problems for installation. Thus it's crucial to evaluate its influence on the physics analysis to determine its necessity. A comparison between the detector with and without SET subdetector was performed in this note. First in single muon particle gun simulation to evaluate the track and energy reconstruction performances and various efficiencies, then in Higgs mass reconstruction in two benchmark events with di-muon final states:  $ZH$  recoil(recoil mass of  $\mu^+\mu^-$  pairs from  $Z \rightarrow \mu^+\mu^-$ ) and  $\nu\nu H, H \rightarrow \mu^+\mu^-$  (invariant mass).

## 2 Software and Sample

The software for simulation is Mokka(Modellierung mit Objekten eines Kompakten Kalorimeters, Object Modeling for Compact Calorimeters) and reconstruction is Marlin. Both of them are Geant4 based.

41 The newly developed Mokka specifically for CEPC is also called MokkaC. MokkaC is a Monte-Carlo  
 42 simulation tool that can either take built-in particle gun or input files as event generators and simulates  
 43 the subsequent processes in the detector. The purpose of simulation is essentially to provide test samples  
 44 for reconstruction. Marlin is a modular reconstruction framework that runs multiple processors, each  
 45 deals with a specific part of reconstruction. And the main categories are: hit digitization, track recon-  
 46 struction and particle identification(PID). The user can switch any processor to a new one as long as they  
 47 match in I/O.

48 In each single muon particle gun simulation,  $5 \times 10^6$  muons with fixed energy are shot in random  
 49 directions. There are 5 criteria for track reconstruction performances. They are:

50  $D_0$ : The shortest distance between the reconstructed track and the gun position( in this case the IP)  
 51 in the  $xy$  plane.

52  $Z_0$ : The shortest distance between the reconstructed track and the gun position along  $z$  axis.

53  $\theta$ : The angle between the momentum direction and  $z$  axis.

54  $\phi$ : The angle of the momentum direction in  $xy$  plane.

55  $\Omega$ : Signed curvature of the track.

56 For  $\theta$ ,  $\phi$  and  $\Omega$ , the performances are evaluated by the difference between the reconstructed values and  
 57 the real values(simulated values). In addition, muon energy reconstruction precision and SET efficiency  
 58 are calculated, the latter is defined by:

$$\epsilon_{\text{trk}} = \frac{\text{Number of reconstructed tracks with SET hits}}{\text{Number of reconstructed tracks passed through SET}}$$

59 Each of the other two simulations contains  $10^4$  Higgs events. The feynman diagram for  $ZH$  recoil is  
 60 shown in Figure 2.

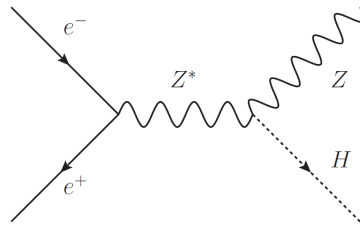


Figure 2:  $ZH$  recoil

61 In  $\nu\nu H, H \rightarrow \mu^+ \mu^-$  events, the muon-anti muon candidates are selected by two muons(one muon and  
 62 one anti muon) carrying largest amount of energies. The invariant mass, i.e. the Higgs mass, is calculated  
 63 by

$$M_{\mu\mu} = \sqrt{(E_{\mu^-} + E_{\mu^+})^2 - (p_{\mu^-} + p_{\mu^+})^2}$$

64 In  $ZH$  recoil events, the leptons carrying more than 25GeV of energy are selected as candidates. And  
 65 di-muon pairs are selected by the criterion

$$|M_{\mu\mu} - M_Z| < 10\text{GeV}$$

66 In the case of multiple candidate pairs, those with smallest  $|M_{\mu\mu} - M_Z|$  are selected. Then the recoil  
 67 mass(Higgs mass) is calculated by

$$M_{\text{recoil}} = \sqrt{(\sqrt{s} - E_{\mu^-} - E_{\mu^+})^2 - (p_{\mu^-} + p_{\mu^+})^2}$$

## 3 Results

All of the result figures are in Section 5.

### 3.1 Single Muon

Figure 3~7 show the distribution of 5 track reconstruction performance criteria with and without SET subdetector at 50GeV. All of them show normal reconstruction performance with notable differences between some pairs. The SET covers from -0.79 to 0.79 on the horizontal axis.

To quantify the results, each diagram was sliced in  $y$  direction and did gaussian fitting for each slice of data. The results are shown in Figure 8. We can learn that SET does improve  $\sigma(Z_0)$ ,  $\sigma(\theta_{\text{Reco}} - \theta_{\text{MC}})$  and  $\sigma(\Omega_{\text{Reco}} - \Omega_{\text{MC}})$ , while having little effect on  $\sigma(Z_0)$  and  $\sigma(\phi_{\text{Reco}} - \phi_{\text{MC}})$ .

You can do this with various energies and choose a benchmark point in the diagram to manifest energy dependence. I picked a  $\theta$  angle very close to  $xy$  plane, i.e.  $\cos\theta \approx 0$ , since that's where the most difference is incurred by SET while avoiding the center cathode plate in TPC. Figure 9 shows the energy dependence of the performance at that point has negative correlation and stable at high energies.

Figure 10 shows the muon energy reconstruction performance. And since SET only covers the barrel area, the same thing only using tracks go through the area are also presented. Figure 11 is for SET efficiency, and Figure 12 is PID efficiency. It turns out that SET does little help in PID for muons. As the PID efficiency in SET covered area is already very high ( $\approx 98\%$ ) without SET.

### 3.2 Higgs Events

As shown Table 1, the SET detector increases the energy resolution for Higgs mass by about 22%~24%, similar to the percentage gain in single muon energy reconstruction at high energies. The higgs reconstruction efficiency is almost same regardless of SET. The Higgs signal was fitted with crystal ball function to get  $\sigma$  values.

Table 1:  $\sigma/\text{GeV}$  values for Higgs mass

Settings	$ZH$ recoil	$\nu\nu H, H \rightarrow \mu^+ \mu^-$
With SET	0.32	0.25
Without SET	0.39	0.31
Higgs reconstruction efficiency	81%	91%

## 4 Conclusion

The above results clearly demonstrate that the SET subdetector's impact on the performance is notable. Another thing implied in Figure 10 and 12 is that the reconstruction performance (energy resolution and PID) is higher for tracks gone through SET area, compared to the endcap, even without SET. This might change if we add the Endcap Tracking Detector (ETD), which is the SET's counterpart at the endcap. Right now it's not included in the full detector model. All of these factors have come to make the difference in Higgs mass reconstruction accuracy. The difference is significant and considering it's just a small part of the biggest machine ever built might justify the installation if it's beneficial. However, it's worth noting that had the endcap performance was higher, the accuracy should increase across the board and the difference should be smaller. Which means the ETD will presumably make SET less important. Whether we need to install SET or not should consider all of the above as well as physics involved and practical aspects like cost, structure etc. The  $ZH$  recoil is one of the main higgs production modes in

102 CEPC and the subsequent  $Z \rightarrow ll$ , especially  $Z \rightarrow \mu^+\mu^-$  is most desirable since it covers inclusive Higgs  
 103 channels, produce high precision signals and unlike hadronic decay, no jets are produced. But it also  
 104 suffers from low branching ratio of only around 3.4%, ( also 3.4% for  $Z \rightarrow e^+e^-$ , which is a slightly less  
 105 desirable one, but still better than hadronic decay).  $H \rightarrow \mu^+\mu^-$  also has low branching ratio, but as we  
 106 can see from the results, it too produces high precision signal.

107 Another thing need to be aware is the installation difficulty. The current SET design puts it right  
 108 outside TPC. And it's probably very challenging to do so in reality. We either need a big support structure  
 109 around it, which is probably out of the question inside that cramped area, or install it on the surface of  
 110 the Ecal. If the latter one is chosen, then the SET must need to change its shape accordingly, from near  
 111 circular transverse shape to an octagonal one. And become farther away from TPC. Then the whole  
 112 performance also should be re-evaluated.

## 113 5 Result Figures

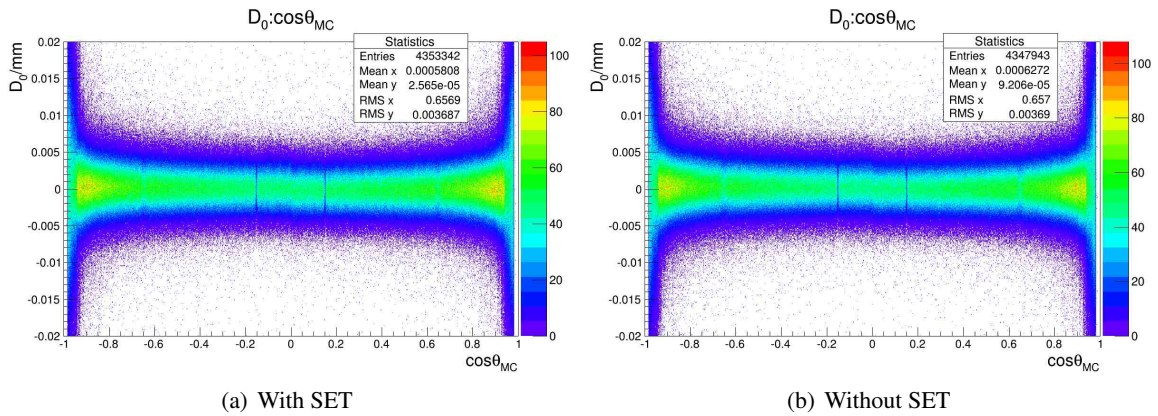


Figure 3:  $D_0$  distribution(50GeV)

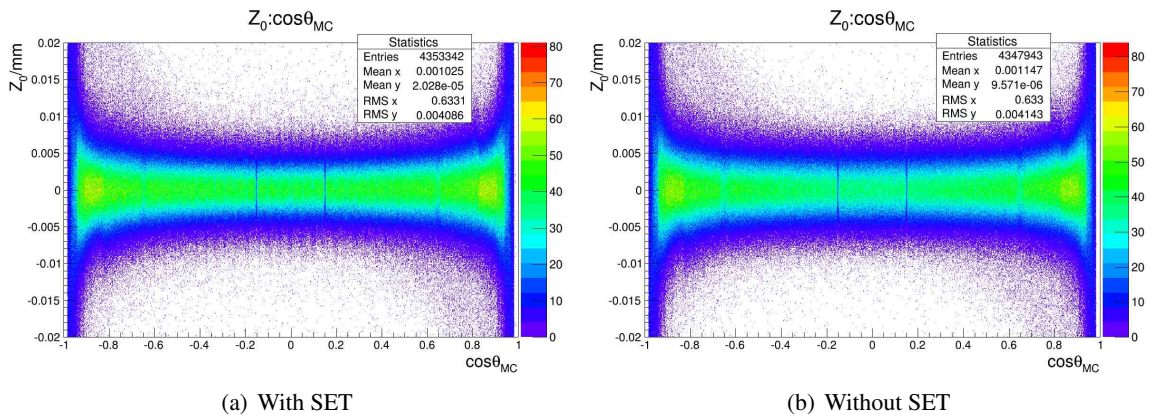


Figure 4:  $Z_0$  distribution(50GeV)

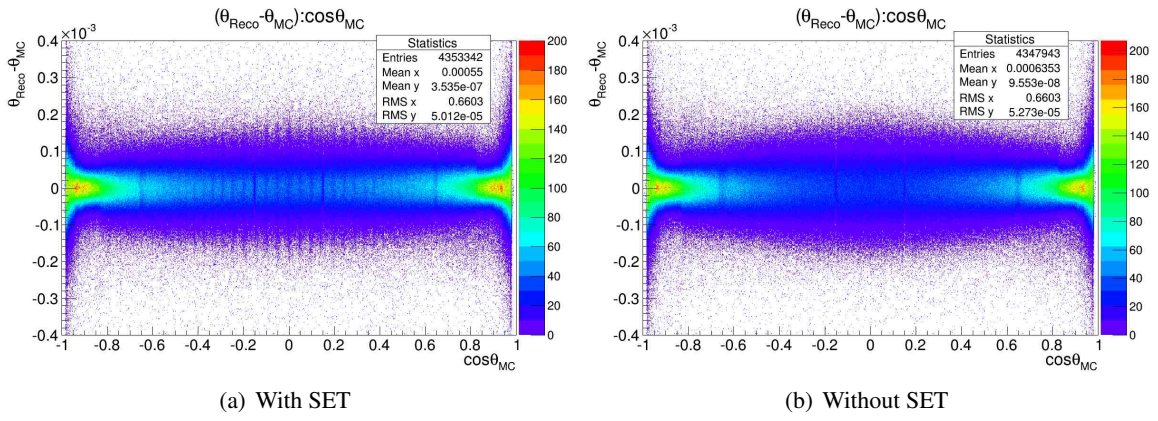


Figure 5:  $\theta_{\text{Reco}} - \theta_{\text{MC}}$  distribution(50GeV)

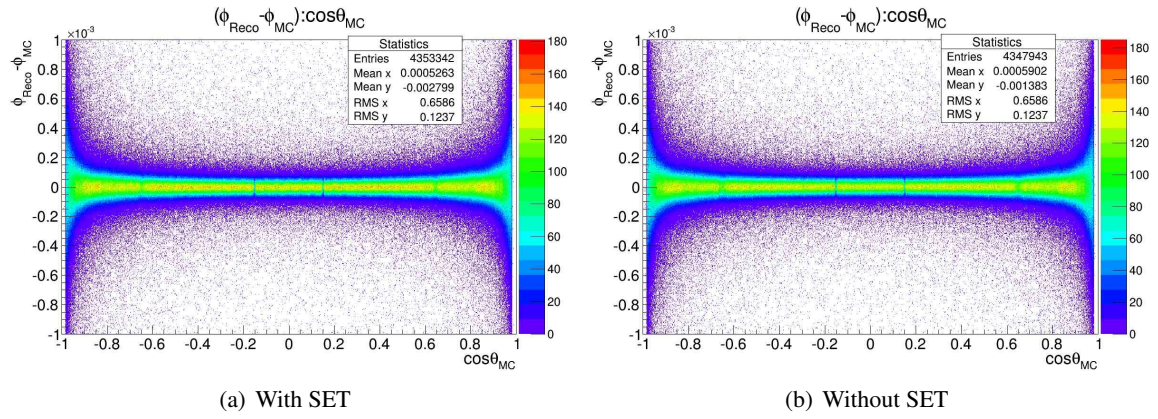


Figure 6:  $\phi_{\text{Reco}} - \phi_{\text{MC}}$  distribution(50GeV)

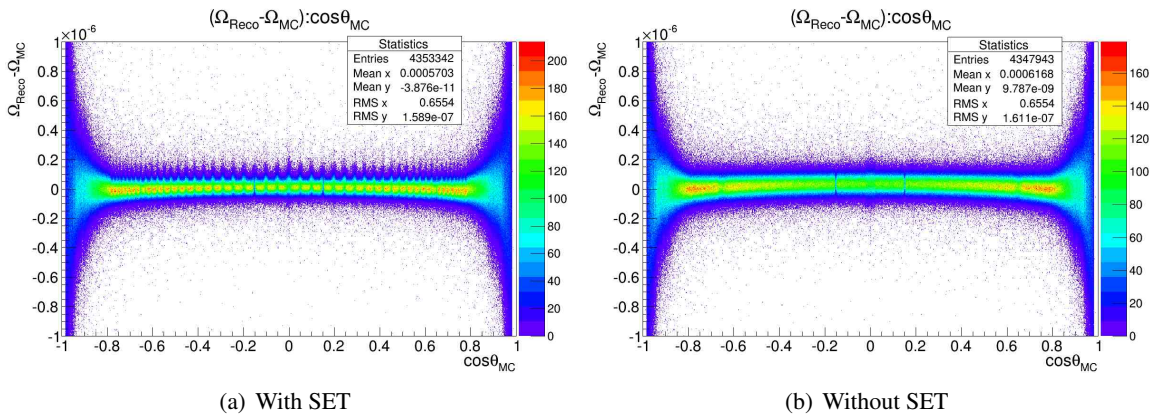


Figure 7:  $\Omega_{\text{Reco}} - \Omega_{\text{MC}}$  distribution(50GeV)



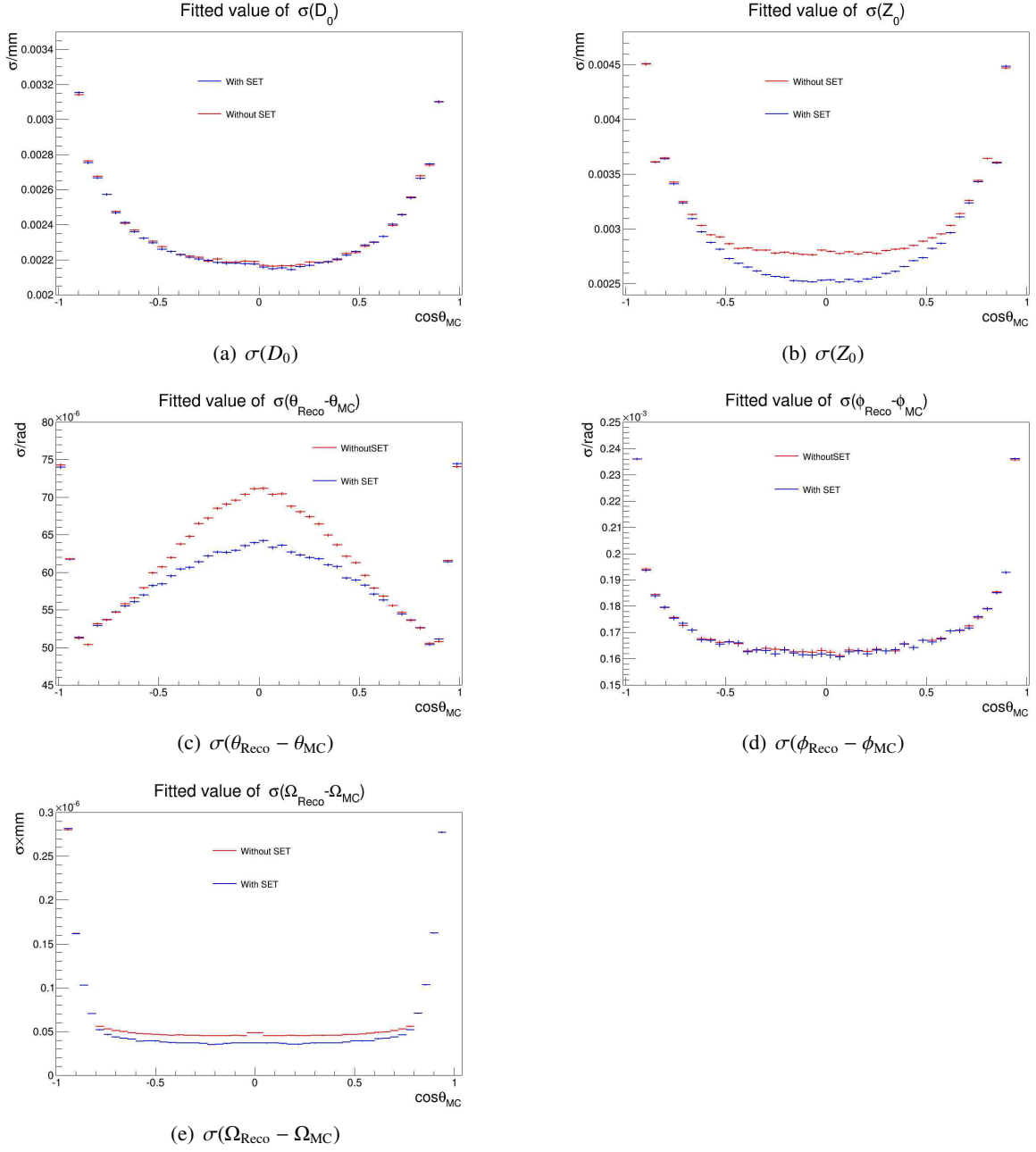
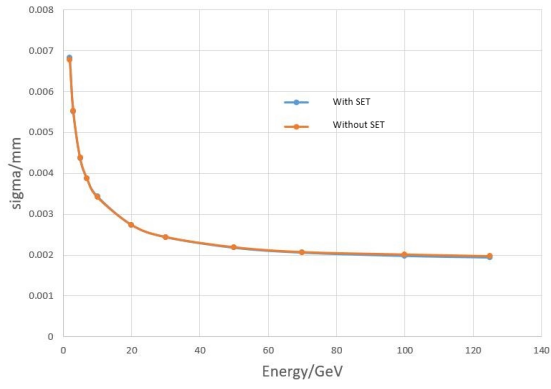
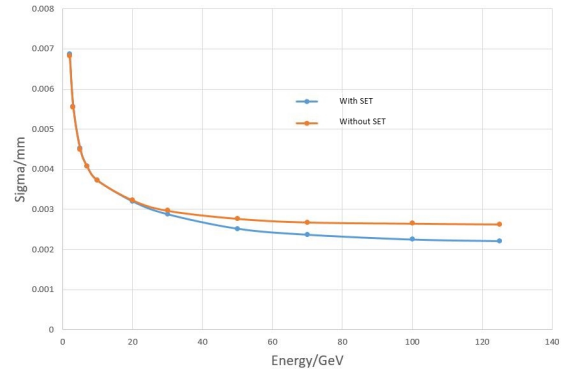


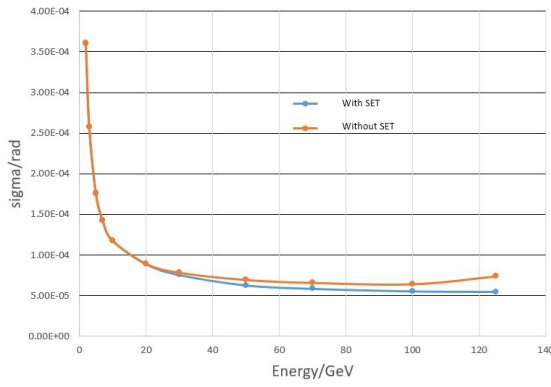
Figure 8: Fitted values(50GeV)



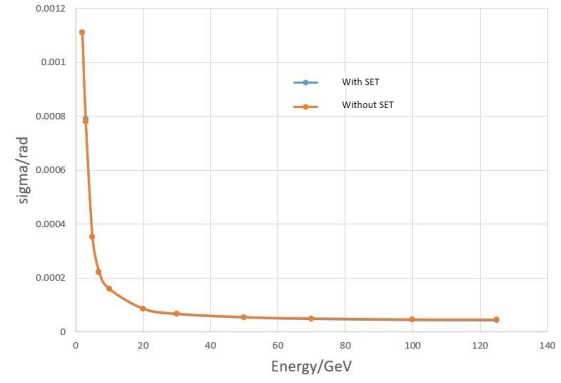
(a)  $\sigma(D_0)$



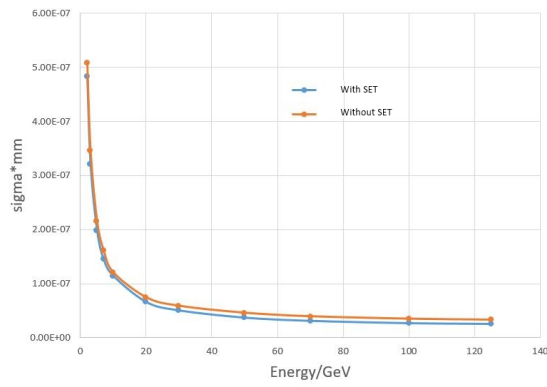
(b)  $\sigma(Z_0)$



(c)  $\sigma(\theta_{\text{Reco}} - \theta_{\text{MC}})$



(d)  $\sigma(\phi_{\text{Reco}} - \phi_{\text{MC}})$



(e)  $\sigma(\Omega_{\text{Reco}} - \Omega_{\text{MC}})$

Figure 9: Energy dependence of fitted values at  $\cos\theta \approx 0$

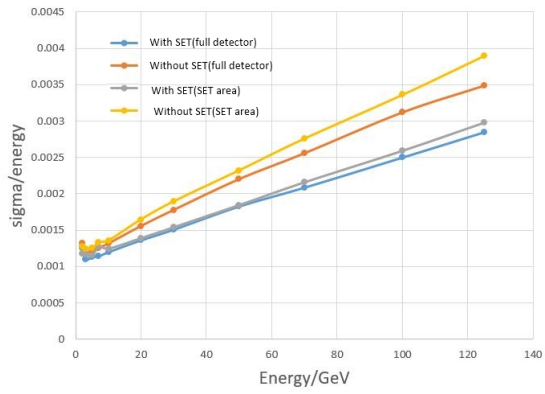


Figure 10:  $\sigma(E)/E$

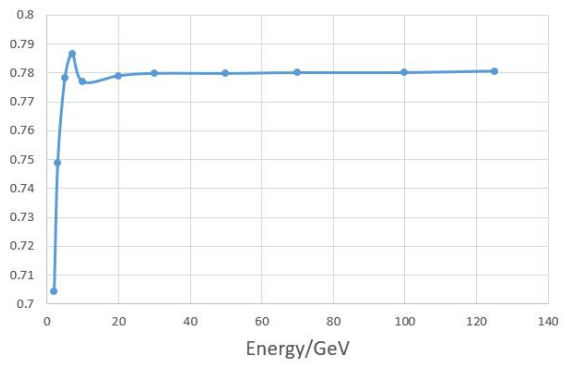


Figure 11:  $\epsilon_{\text{trk}}$

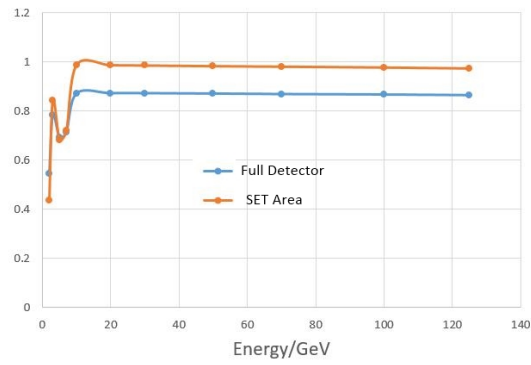


Figure 12: PID efficiency

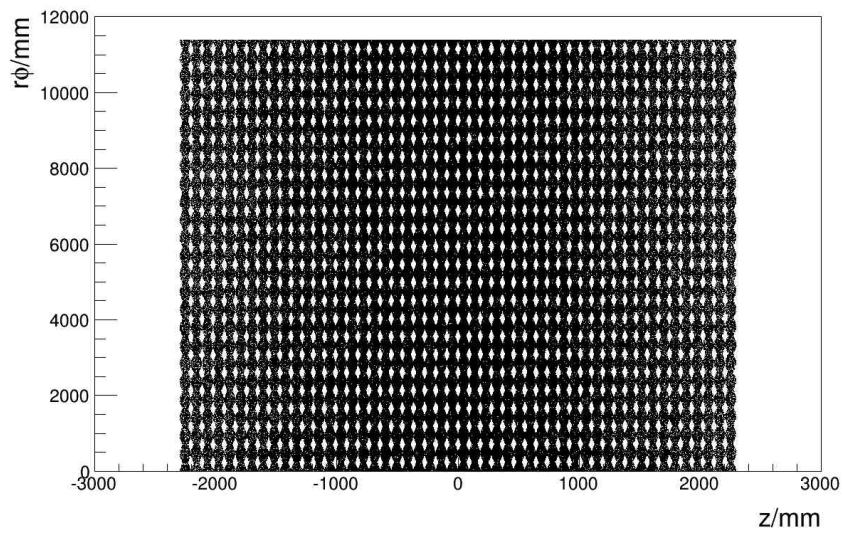


Figure 13: Reconstructed hitmap on SET